Full Paper
doi.org/10.1002/ejic.202000422

Tetrapnictide Dianions

Isomerism and Biradical Character of Tetrapnictide Dianions: A Computational Study

Peter Coburger,*[a,b] Robert Wolf,[a] and Hansjörg Grützmacher*[b]

Abstract: We present a computational study on tetrapnictide dianions Pn_4^{2-} (Pn = P, As, Sb, Bi), using density functional theory (DFT), coupled-cluster [DLPNO-CCSD(T)] and complete active space self-consistent field (CASSCF) methods. Environmental effects such as solvation and coordination of counterions are included. The calculations reveal that out of three isomers (square-planar, butterfly and capped-triangle), the square planar isomers are generally the most stable. The counterion (Li^+ and Mg^{2+}) used in the calculations have a substantial effect on the relative stabilities. The square planar isomers show considerable biradical character. Calculated reactions toward alkenes indicate that this unusual electronic structure has significant implications on the reactivity of the Pn_4^{2-} dianions.

Introduction

Square-planar tetrapnictide dianions, Pn_4^{2-} (Pn = P, As, Sb, Bi, Figure 1), are unusual, four-membered heterocycles containing a 6π-electron system. The first example, Bi_4^{2-}, was synthesized by Corbett and co-workers in 1977.[1] Since then, several syntheses and solid-state structures of Pn_4^{2-} dianions have been published.[2] Pn_4^{2-} dianions have also been the subject of a number of theoretical studies focusing on the aromaticity of these heterocycles and the investigation of sandwich complexes.[2f,3] Notably, Korber and co-workers coined the term "lone-pair aromaticity" when describing the electronic structures of P_4^{2-} and As_4^{2-}.[2f] The square-planar structure **A** is experimentally observed for all Pn_4^{2-} dianions.[1,2] Calculations revealed that other (hypothetical) isomers are conceivable, specifically the butterfly **B** and the capped triangle **C** (Figure 1).[3a,3b,3f] The stability of the isomers decreases in the order **A** > **B** > **C**.

Related to Pn_4^{2-} dianions are four-membered ring species **1**–**5**, which likewise have a planar structure of the ring comparable to **A** and a 6π electron count (Figure 1).[4] Computational and experimental studies have revealed the substantial open-shell singlet character of these species. Such *singlet biradicaloids* combine comparatively high stability with radical reactivity, which has been exploited for bond activation reactions. Consequently, singlet biradicals have been proposed as catalysts with transition-metal like behavior.[5]

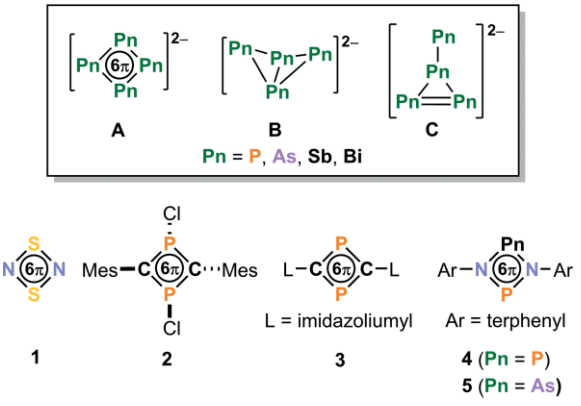

Figure 1. Possible isomers of tetrapnictide dianions (top) and examples of four-membered heterocyclic biradicaloids (bottom).

N_2S_2 (**1**) is a textbook example of a binary p-block element biradicaloid with pronounced singlet biradical character.[6] Further studies revealed that phosphorus is particularly versatile at stabilizing a biradicaloid structure as observed in compounds **2**–**5** synthesized by the groups of Niecke, Schulz and Grützmacher.[4a,4d–4j] The biradicaloid nature of these species has a crucial impact on their reactivity, enabling reactions of **3** and **4** with dihydrogen, chalcogens, diselenides and various multiple-bonded compounds such as alkenes and alkynes. Additionally, **4** has shown promising results in the activation of small molecules such as carbon dioxide and ammonia.[4f]

In analogy to the above-mentioned examples, it is tempting to speculate whether tetrapnictide dianions Pn_4^{2-} might also display significant biradical character. Surprisingly, this question has remained largely unexplored. A previous study by Tuono-

[a] Dr. P. Coburger, Prof. Dr. R. Wolf
University of Regensburg, Institute of Inorganic Chemistry,
93040 Regensburg, Germany
[b] Dr. P. Coburger, Prof. Dr. H. Grützmacher
ETH Zurich, Laboratory of Inorganic Chemistry,
8093 Zürich, Switzerland
E-mail: pcoburger@inorg.chem.ethz.ch
hgruetzmacher@ethz.ch
https://gruetzmacher.ethz.ch/

Supporting information and ORCID(s) from the author(s) for this article are available on the WWW under https://doi.org/10.1002/ejic.202000422.

Part of the German Chemical Society ADUC Prizewinner Collection

Full Paper
doi.org/10.1002/ejic.202000422

nen reported a CASSCF calculation including all valence electrons and orbitals (22 electrons in 16 orbitals) on the $\mathbf{P_4^{2-}}$ dianion and concluded from qualitative metrics that it displays a lower biradical character than the isoelectronic $\mathbf{Se_4^{2+}}$ cation. To the best of our knowledge this is the only study published so far on this issue.[6b] Here, we report a comprehensive theoretical study of the tetrapnictide dianions, which is designed to close this apparent gap in the literature. First, we discuss the stability of different $\mathbf{Pn_4^{2-}}$ isomers. Second, we analyze the biradical character of the square-planar 6π-electron species **A** and their magnesium complexes. Third, quantum chemical studies are also used to generate valuable insight into the potential reactivity of these molecules toward σ- and π-bonds.

Results and Discussion

Isomer Structures of Tetrapnictide Dianions and their $[Li(NH_3)_2]^+$ and $[Mg(NH_3)_x]^{2+}$ (x = 2–4) Complexes

Previous quantum chemical calculations on $\mathbf{Pn_4^{2-}}$ isomers were conducted on isolated molecules.[3a,3b,3f] As environmental effects such as solvation and/or cation interactions might have important implications for such highly charged and small anions, the energetic ordering of the isomers **A**, **B**, and **C** was reinvestigated. The uncoordinated $\mathbf{Pn_4^{2-}}$ isomers **A**–**C** (Figure 1) were calculated. In addition, the coordination of counterions was modeled by including coordination of two $[Li(NH_3)_2]^+$ ions (**A-Li**, **B-Li**, **B-Li′**, **C-Li** and **C-Li′**) and one $[Mg(NH_3)_x]^{2+}$ ion [**A-Mg(NH$_3$)$_x$**, **B-Mg(NH$_3$)$_x$** and **C-Mg(NH$_3$)$_x$**, x = 2, 3 and 4, Figure 2, see the SI for a depiction of all optimized structures]. Here, **B-Li** and **B′-Li** as well as **C-Li** and **C-Li′** differ in the coordination of the lithium cations. All of these ion pairs were investigated using an implicit solvation model for ammonia[7] which was chosen as solvent and co-ligand since tetrapnictide dianions have been experimentally observed in liquid ammonia or related solvents such as ethylene diamine.[1,2] Additionally, to estimate the role of solvation, each ion pair was also investigated in the isolated state. Initial calculations also included the hypothetical $\mathbf{N_4^{2-}}$ ion, whose stability was predicted in an earlier study.[8] However, as soon as counterions and explicit solvation effects are considered that species was found to be unstable towards the decomposition to dinitrogen (see the SI). Furthermore, in agreement with previously reported results, the capped triangle isomer **C** was found to be high in energy regardless of the considered environmental effects such as solvation or coordination of metal cations. Thus, we consider it to be irrelevant for the chemistry of tetrapnictide dianions.

The calculated structures of the tetrapnictide species [**A**, **A-Li** and **A-Mg(NH$_3$)$_x$**] which contain the square-planar $\mathbf{Pn_4^{2-}}$ dianion are in good agreement with the available experimental data (see the SI). In particular, the symmetry of the dianion **A** is very close to D_{4h}, and for all the investigated lithium and magnesium complexes of **A** the deviation from planarity is small (see the SI). The obtained relative stability of the isomers **A**, **B**, and **C** and the respective lithium species is summarized in Table 1. The square-planar isomer **A** is the global minimum for all dianions, regardless whether the calculations were carried out on the isolated species or with a solvent model. However, the square-planar isomer becomes less favored over the butterfly isomer when descending the group. A similar trend was also observed in calculations on a series of neutral X_2Y_2 species (X = N, P, As, Y = O, S, Se, Te) which are isoelectronic to the tetrapnictide dianions.[9] For this series, the authors explained this trend by the general observation that elements with larger atomic size can stabilize acute bond angles more easily which applies for the tetrapnictide dianions as well (e.g. Bi–Bi–Bi in **A** is 90° and 58 and 61° in **B**, see the SI for a detailed comparison). In addition, it was pointed out that butterfly structures of type **B** in the X_2Y_2 species do not contain a π-system, but one more σ-bond than the square-planar isomers.[9] Our calculations also confirm this observation for the tetrapnictide dianions. Here, the Mayer Bond Orders (MBO) within the square-planar isomers **A** clearly indicate the presence of attractive π-bonding, whereas the MBO for the five bonds in the butterfly isomers **B** are close to 1.0 (see the SI for a discussion and a comparison of metrical parameters). Thus, these values suggest the sole presence of σ-bonds in **B**. Therefore, the general preference of heavy elements for single bonds leads to a decreasing energy difference between the butterfly and the square-planar structure and for Pn = Sb or Bi, **B** is only few kcal mol^{-1} less stable than **A** (see Table 1).

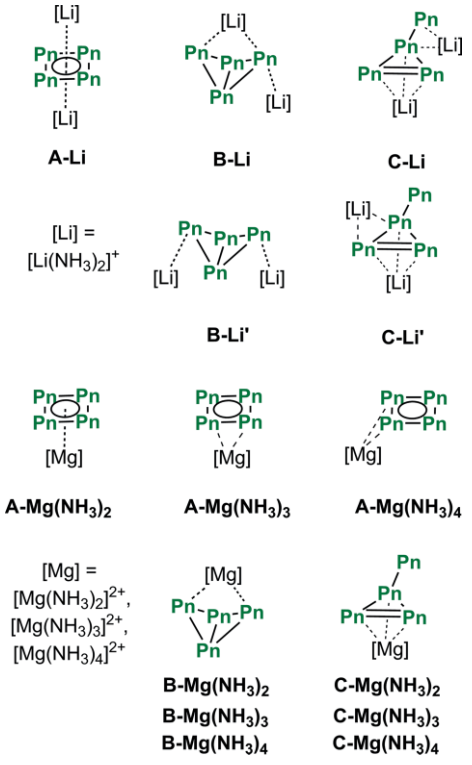

Figure 2. Investigated lithium and magnesium complexes of tetrapnictide dianions and their lithium and magnesium complexes (Pn = P, As, Sb, Bi).

Similar results for the bonding in **A** and **B** have been obtained when the species coordinated to Li^+ or Mg^{2+} were investigated (see the SI). Interestingly, the stabilization of **B** with respect to **A** increases the most when going from As to Sb for the uncoordinated dianions and also in most cases for the lithium and magnesium species. This might be explained by the

Full Paper
doi.org/10.1002/ejic.202000422

Table 1. Gibbs free energies of tetrapnictide species [PBE0-D3BJ/def2-TZVPP CPCM(ammonia), in kcal mol^{-1} at 298 K]. **B** and **C** are referenced against **A** and the lithium species are referenced against **A-Li**, respectively. Values in parentheses refer to the respective energies in the isolated non-solvated state.

Pn	B	C	B-Li	C-Li	B-Li′	C-Li′
P	17.3 (20.8)	37.2 (32.3)	7.0 (18.1)	30.9 (42.7)	13.0 (31.3)	31.0 (41.4)
As	14.5 (18.5)	42.5 (37.4)	3.3 (15.3)	36.0 (49.9)	7.8 (29.5)	37.8 (48.7)
Sb	6.6 (11.1)	40.7 (35.2)	−3.0 (10.8)	33.9 (49.4)	0.2 (23.6)	35.6 (48.3)
Bi	2.6 (7.1)	40.2 (34.3)	−6.3 (7.1)	33.9 (48.6)	−1.4 (19.3)	35.8 (47.5)

change of the electron affinity of the pnicogens when descending the row which follow the trend (P: 17.2, As: 18.6, Sb: 24.2, Bi: 21.7, values in kcal mol^{-1}).[10] Since the anionic charge in **B** is rather localized being mostly distributed over two atoms rather than four in **A**, elements with a particularly high electron affinity might stabilize these structures better.

The isomers **B-Li** and **Bi-Li′** show a significant difference in their Gibbs energies, with **B-Li** being favored for all considered pnicogens (Table 1). This can be explained with the orientation of the lone pairs of electrons at the negatively charged pnicogen centers in **B** (see the SI for a graphical representation), which allow **B** to act as a chelating ligand via these two atoms. Looking at the energies of **B-Li** compared to **A-Li**, the butterfly isomer is favored for the heavier congeners (Pn = Sb and Bi) when a solvent model is included. These results disagree with the experimental data, since all observed square-planar dianions **A** have been prepared with two monocations as counterions so far.[1,2] This may indicate that in a highly polar solvent, such as ammonia, the simultaneous coordination of *two* monocations at the tetrapnictide dianions is unlikely and a solvent separated ion pair might be present. Therefore, the lithium species chosen in this study might not be suitable to describe the chemistry of the tetrapnictide dianions in solution.

For the magnesium species **A-Mg(NH$_3$)$_x$** (x = 2–4), the solvent model has a considerable effect on the geometries. For x = 2, the dianion **A** acts as an η^4 ligand with almost equal Mg–Pn distances. For x = 3 the dianion still acts as an η^4 ligand, however, two Mg–Pn distances are significantly elongated now. Finally, for x = 4, the dianion acts as an η^2 ligand. In contrast, the η^4 coordination with similar Mg–Pn distances is observed in the isolated state for all x = 2–4. For the non-coordinated dianions, the square-planar isomer **A** is significantly more stable than the butterfly isomer **B**. In the case of the magnesium complexes, the butterfly species **B-Mg(NH$_3$)$_x$** are considerably stabilized with respect to **A-Mg(NH$_3$)$_x$** (Table 2). Except for Pn = P (x = 2–4) and As (x = 4), **B-Mg(NH$_3$)$_x$** is even favored over **A-Mg(NH$_3$)$_x$** in most cases. Here, the already discussed chelating properties of **B** might cause a higher interaction energy with the magnesium center than **A**. Finally, when the change of Gibbs free energy associated with the change of the number of ammonia molecules coordinated to magnesium is taken into consideration, the following global minima are obtained: **A-Mg(NH$_3$)$_4$** for Pn = P and As; **B-Mg(NH$_3$)$_2$** for Pn = Sb and Bi (see the SI).

Overall, our results show that the inclusion of solvation has an impact on the energetic ordering of the isomers **A** and **B** as well as for the structures of **A-Mg(NH$_3$)$_x$**.

Biradical Character of Square-Planar Tetrapnictide Dianions and their Tetramminemagnesium Complexes

Next, we discuss the biradical character of the square-planar isomers which might be relevant for the reactivity of these dianions, namely **A** (for Pn = P, As, Sb and Bi) and their magnesium complexes **A-Mg(NH$_3$)$_4$** (for Pn = P and As). The latter have been chosen since they are the global minimum for all investigated magnesium species in the case of Pn = P and As. For completeness, the species **A-Li** have been investigated as well showing a biradical character similar to **A** (see the SI). In typical four-membered biradicaloids with 6π-electrons such as **1**, two biradical Lewis structures can be formulated (Figure 3).[6e] Several methods have been developed to evaluate the contribution of such radical Lewis structures to the overall electronic structure and the associated biradical character. CASSCF calculations have been used extensively and were also utilized to analyze **1**.[6b] The results of such calculations show that structure **I** contributes much more strongly than **II** to the overall electronic structure of **1**. Similar results were also obtained for the more recently discovered species **3**–**5**.[4e,4i]

As shown in Figure 3, equivalent Lewis structures can be formulated for **A** and **1**. However, **A** shows higher symmetry than **1** (D_{4h} for **A** vs. D_{2h} for **1**), hence, **A-I** and **A-II** contribute equally to the overall electronic structure. In the *side-on* coordinated species **A-Mg(NH$_3$)$_4$** the symmetry is again lowered, however, **A-I** and **A-II** both still contribute significantly to the overall electronic structure (vide infra). As the potential biradical character in **A** and **A-Mg(NH$_3$)$_4$** is expected to occur within

Table 2. Gibbs free energies of tetrapnictide species [PBE0-D3BJ/def2-TZVPP CPCM(ammonia), in kcal mol^{-1} at 298 K]. The coordinated isomers **B-Mg(NH$_3$)$_x$** and **C Mg(NH$_3$)$_x$** are referenced against **A-Mg(NH$_3$)$_x$** (x = 2–4), respectively. Values in parentheses refer to the respective energies in the non-solvated isolated state. Note that no stable structures for **C-Mg(NH$_3$)$_2$** for Pn = Sb and Bi could be found, rather the butterfly isomers were obtained after a geometry optimization.

Pn	B-Mg(NH$_3$)$_2$	C-Mg(NH$_3$)$_2$	B-Mg(NH$_3$)$_3$	C-Mg(NH$_3$)$_3$	B-Mg(NH$_3$)$_4$	C-Mg(NH$_3$)$_4$
P	1.1 (1.2)	42.1 (46.0)	0.6 (8.1)	33.5 (41.6)	6.0 (2.6)	36.0 (35.3)
As	−2.3 (−2.0)	50.0 (52.1)	−2.5 (4.9)	39.1 (47.8)	4.5 (−1.9)	42.9 (41.4)
Sb	−7.9 (−7.3)	–	−0.7 (0.0)	42.6 (44.6)	−1.0 (−6.8)	39.6 (39.4)
Bi	−10.4 (−9.7)	–	−4.1 (−2.9)	42.2 (44.3)	−4.3 (−8.7)	39.4 (40.9)

Full Paper
doi.org/10.1002/ejic.202000422

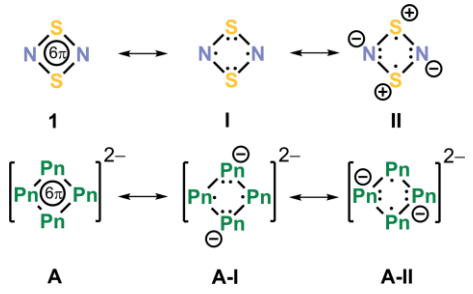

Figure 3. Biradicaloid Lewis structures of **1** and **A**. (Pn = P, As, Sb, Bi). For clarity, only the electrons contributing to the π-systems in **1** and **A** are shown.

the 6π-system, CASSCF calculations with an active-space of six electrons in four orbitals [CASSCF(6/4)] were conducted. The resulting orbitals comprising the π-system of those dianions are exemplarily shown for $\mathbf{P_4^{2-}}$ and its magnesium complex in Figure 4. In the free dianion **A**, the orbitals π_2 and π_3 are degenerate, while in **A-Mg(NH$_3$)$_4$** the 6π-system is polarized due to the presence of the magnesium center which lifts the degeneracy of π_2 and π_3. Still, in both species these two orbitals show a transannular antibonding interaction while π_4 exhibits transannular bonding interactions only. Since the population of π_4 is small compared to the population of π_2 and π_3, this results in an overall antibonding transannular interaction in **A** and **A-Mg(NH$_3$)$_4$**. This finding is underpinned by a topology analysis of the CASSCF electron density of **A** and **A-Mg(NH$_3$)$_4$** which confirms the absence of a bond critical point between transannular pnicogen atoms (see the SI). Having this topology analysis in hand, it was also possible to confirm the aromaticity of **A** by calculating the Shannon aromaticity index (SAI).[11] Here, the calculated values range from 1.5×10^{-7} ($\mathbf{P_4^{2-}}$) to 6.2×10^{-6} ($\mathbf{Bi_4^{2-}}$) which indicates a somewhat lower aromaticity than reported in the archetypal benzene molecule (SAI = 1.7×10^{-8}).[11] However, the SAI for all tetrapnictides are still well below the critical value of 0.003, thus confirming their aromaticity.

When the active orbitals are expressed as natural orbitals (as shown in Figure 4), the final CASSCF wavefunctions can be written as the weighted sum of the ground-state configuration-state function (CSF) and two double-excited CFS's according to Equation (1).

$$\Psi = c_0|\pi_1^2\pi_2^2\pi_3^2\pi_4^0> + c_1|\pi_1^2\pi_2^0\pi_3^2\pi_4^2> + c_2|\pi_1^2\pi_2^2\pi_3^0\pi_4^2> \quad (1)$$

Here, $|\pi_1^2\pi_2^2\pi_3^2\pi_4^0>$ denotes a CFS with the first three π-orbitals of the active-space doubly occupied; the other configuration-state functions are defined accordingly. In typical biradicaloids – such as ozone and also **1**–**5** - only one double excitation contributes significantly to the biradical character.

Several expressions based on c_1 have been derived to quantify that character.[12] However, as Tuononen and co-workers pointed out in their study of tetrachalcogen dications, such equations are not valid when two excitations contribute significantly to the biradical character.[6b] Still, the coefficients c_1 and c_2 can be used as a qualitative measure, since larger coefficients are associated with a higher biradical character. Similarly, the occupation of the orbital π_4 is linked to the biradical character.

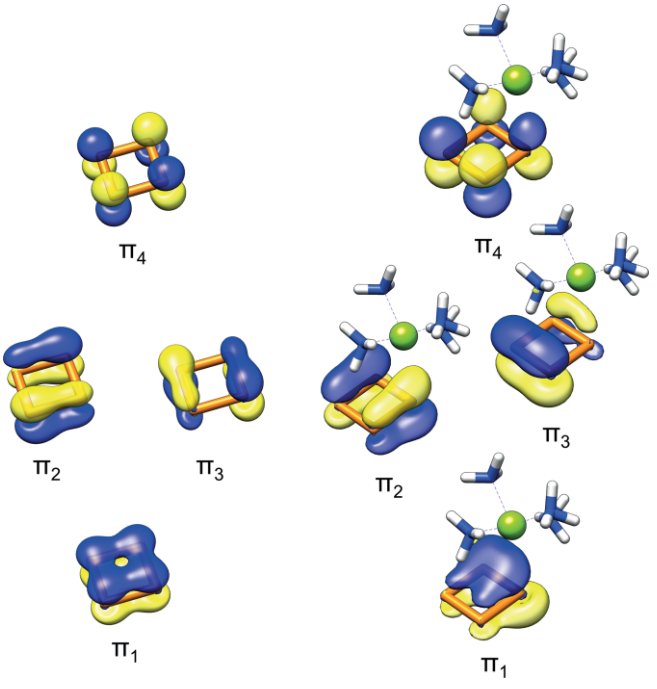

Figure 4. Natural orbitals representing the π-system of $\mathbf{P_4^{2-}}$ and **A-Mg(NH$_3$)$_4$** (Pn = P) obtained from a CASSCF(6/4) calculation. Surface isovalue = 0.05.

Table 3 summarizes the CASSF data. The results clearly show that the biradical character of the $\mathbf{Pn_4^{2-}}$ dianions increases when going down the group. It is noteworthy that the biradical character of $\mathbf{As_4^{2-}}$ is comparable with N_2S_2 [**1**, occ(π_4) = 0.150, c_1^2 = 6.8 % and c_2^2 = 0.6 %], while those of $\mathbf{Sb_4^{2-}}$ and $\mathbf{Bi_4^{2-}}$ exceed that of **1**. For **A-Mg(NH$_3$)$_4$** the contributions of c_1^2 and c_2^2 are lower than in the free dianions and consequently their biradical character is smaller. The use of localized orbitals as active orbitals in the CASSCF calculation additionally allows for a direct interpretation of the resulting wavefunction in terms of Lewis structures (see Figure 3 and the SI for details). Such an analysis reveals that biradicaloid structures **A-I** and **A-II** in total contribute more than 40 % to the overall wavefunction of **A** ($\mathbf{P_4^{2-}}$ 40.8 %, $\mathbf{As_4^{2-}}$: 43.2 %, $\mathbf{Sb_4^{2-}}$: 44.8 %, $\mathbf{Bi_4^{2-}}$: 46.6 %). Due to the lower biradical character, **A-I** and **A-II** contribute less to the wavefunction in **A-Mg(NH$_3$)$_4$** (P: 35.2 %, As: 34.2 %). For N_2S_2 (**1**) contributions of 33.8 % for **I** and 11.9 % for **II** were calculated using the same procedure. This finding is consistent with the CASSCF(22/16) results of Tuononen and co-workers and valence-bond theory (VB) calculations on N_2S_2, which estimate the total contribution of **I** and **II** between 40 % and 54 %.[6b,6c,6e,6g] These findings

Table 3. π-Orbital occupations of **A** obtained from CASSCF(6/4) calculations and sum of squared CI-coefficients c_1 and c_2 [according to Eq (1)]. The data for the magnesium species **A-Mg(NH$_3$)$_4$** (for P and As) are given in parentheses; due to the non-degeneracy of π_2 and π_3, individual values for the sum of squared CI-coefficients c_1 and c_2 are given. The occupation of π_1 for all investigated species is very close to 2 (> 1.99).

	$\mathbf{P_4^{2-}}$	$\mathbf{As_4^{2-}}$	$\mathbf{Sb_4^{2-}}$	$\mathbf{Bi_4^{2-}}$
π_2	1.946 (1.962)	1.930 (1.962)	1.922	1.908
π_3	1.945 (1.941)	1.930 (1.918)	1.920	1.906
π_4	0.110 (0.097)	0.141 (0.121)	0.159	0.187
$c_1^2 + c_2^2$	5.4 % (2.9 %, 1.9 %)	7.4 % (4.1 %, 1.9 %)	7.9 %	9.3 %

Full Paper
doi.org/10.1002/ejic.202000422

support our approach and justify the use of an active-space of six electrons in four orbitals to analyze the biradical character in **A** and **A-Mg(NH$_3$)$_4$**. Based on these data, square-planar tetrapnictides **A** can be described as biradicaloids with similar biradical character as N_2S_2 (**1**).

Reactivity of Square-Planar Tetrapnictide Dianions and their Tetramminemagnesium Complexes

In order to assess the potential impact of the assumed biradical character on the reactivity, model reactions of **A** and **A-Mg(NH$_3$)$_4$** with dihydrogen, ethene and tetrafluoroethene [Scheme 1 (a)] were studied computationally by DFT using the same method as for the analysis of the isomers (see the Computational Details). Since the tetrapnictides are often handled in liquid ammonia (b.p. 240 K), the Gibbs free energies were calculated at 240 K using a solvent model for ammonia (Table 4). The

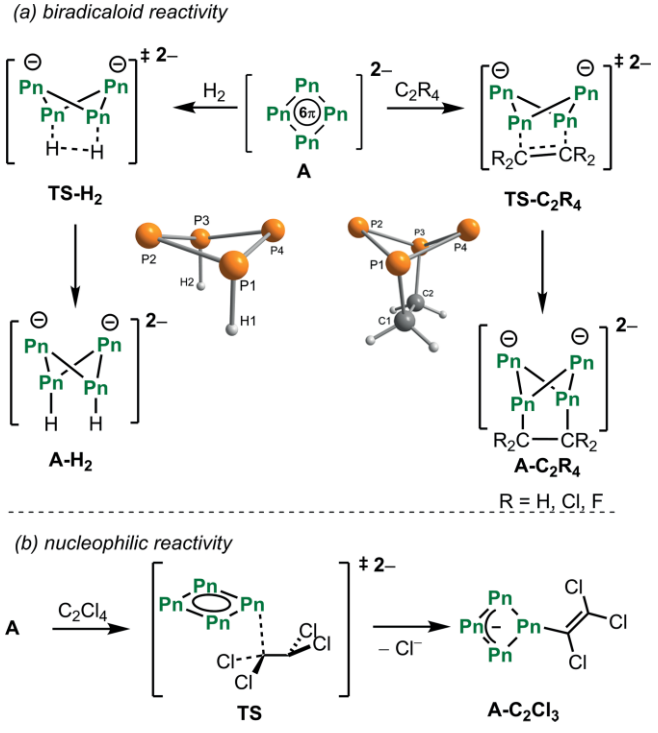

Scheme 1. (a) Mechanism of the biradical-type activation of dihydrogen and alkenes by square-planar tetrapnictide dianions (Pn = P, As, Sb, Bi). The calculated structure of two of the products [**A-H$_2$** (left) and **A-C$_2$H$_4$** (right) for Pn = P] is shown as an example; selected bond lengths [Å] and angles [°]: **A-H$_2$**: P1–P2 2.208, P2–P3 2.207, P3–P4 2.206, P4–P1 2.207, P1–H1 1.444, P1–P2–P3 85.74, P4–P1–P2 90.12; **A-C$_2$H$_4$**: P1–P2 2.212, P2–P3 2.213, P3–P4 2.212, P4–P1 2.211, P1–C1 1.882, P1–P2–P3 78.44, P4–P1–P2 89.86, P1–C1–C2 109.57. (b) Nucleophilic reactivity towards tetrachloroethene.

reaction of ammonia solvated **A** with both hydrogen (giving **A-H$_2$**) and ethene (giving **A-C$_2$H$_4$**) were calculated to be endergonic, whereas those with the halogenated ethenes (giving **A-C$_2$Cl$_4$** and **A-C$_2$F$_4$**) were exergonic except for the cycloaddition of C_2Cl_4 with Sb_4^{2-} and Bi_4^{2-}. The molecular structures of the products can be described as tetrapnicogen-1,3-diides (**A-H$_2$**) and tetra-pnicogenbicyclo[2.1.1]hexanediides (**A-C$_2$R$_4$**). The structures of **A-H$_2$** and **A-C$_2$H$_4$** are shown for Pn = P as an example in Scheme 1 and metrical parameters of the calculated structures are found in the Supporting Information. All bond lengths are in the range of standard Pn–Pn, Pn–H or Pn–C single bonds (see the SI).

The activation barriers for the reactions between Pn_4^{2-} and hydrogen or ethane decrease in the order Pn = P > As > Sb (Table 4). Thus, the activation barriers follow the trend of increasing biradical character and polarizability in **A** for Pn = P < As < Sb. For Bi_4^{2-}, the poor orbital overlap between the diffuse bismuth orbitals and the small orbitals on hydrogen or carbon, respectively, might explain the small increase in the activation barrier when compared to Sb_4^{2-}. However, in case of the halogenated ethene derivatives, a slight increase of the barriers was found when descending the pnicogen group, but the difference of 1–2 kcal mol^{-1} falls within the reliability of the DFT method.[13] It is noteworthy that the stability of all products decreases from P_4^{2-} to Bi_4^{2-} with the only exception being the reactions with dihydrogen where the product in case of Pn = Sb is slightly more stable than in the case of Pn = As.

Thus, the stability of the products can be tentatively linked to the stability of the resulting Pn–H or Pn–C bonds, which generally decreases when descending the pnicogen group.[14] Furthermore, for each pnicogen, both the transition states and the products are stabilized when going from ethene to tetrachloroethene to tetrafluoroethene. This observation follows the trend of increasing electrophilicity in the ethene derivatives.

The reactivity of the dianions **A** was additionally calculated in their non-solvated isolated state (Table 4, values in parentheses). Here, the same trends as for the solvated dianions are found. However, the calculated activation barriers for the reaction with ethene and tetrafluoroethene are unreasonably low, the extreme case being **TS-C$_2$F$_4$** for Pn = P ($\Delta G^{\ddagger}$ = –1.7 kcal mol^{-1}). This might be explained by the positive HOMO energies of the dianions **A** in the isolated state (P: 4.2 eV, As: 4.1 eV, Sb: 3.1 eV, Bi: 3.2 eV) indicating an unbalanced description of anionic charge which could artificially increase their reactivity. Thus, the inclusion of solvation effects is essential to describe the reactivity of the square-planar dianions **A**. But remarkably, no transition state for the biradicaloid reactivity in

Table 4. Gibbs free energies of calculated transition states and products for the biradicaloid reactivity of **A** and **A-Mg(NH$_3$)$_4$** [PBE0-D3BJ/def2-TZVPP CPCM(ammonia), in kcal mol^{-1}] at 240 K. The sum of the Gibbs free energies of the respective starting materials for each reaction was taken as the reference. Values obtained in the isolated state for the non-solvated dianions **A** are given in parentheses. Values in brackets refer to the energies calculated for **A-Mg(NH$_3$)$_3$**.

	TS-H_2	A-H_2	TS-C_2H_4	A-C_2H_4	TS-C_2Cl_4	A-C_2Cl_4	TS-C_2F_4	A-C_2F_4
P_4^{2-}	31.8 (28.3)	13.8 (12.0)	26.0 (13.9)	0.9 (–5.0)	21.3 (–)	–5.7 (–33.8)	19.3 (–1.7)	–22.6 (–41.8)
As_4^{2-}	30.2 (27.5)	16.3 (14.0)	24.2 (12.9)	5.1 (–1.2)	21.3 (–)	–0.6 (–25.8)	19.3 (0.2)	–17.0 (–33.6)
Sb_4^{2-}	27.2 (26.3)	15.1 (15.1)	20.9 (14.8)	5.6 (3.1)	22.9 (–)	1.5 (–12.4)	21.3 (9.8)	–12.2 (–20.2)
Bi_4^{2-}	28.2 (27.5)	17.9 (17.7)	21.3 (14.3)	11.4 (7.7)	22.4 (–)	2.0 (–11.9)	21.3 (9.9)	–8.2 (–15.5)
P_4-Mg$(NH_3)_4$	37.4 [28.3]	14.0 [7.2]	32.3 [21.5]	–1.6 [–8.1]	33.1 [24.4]	–3.1 [–7.6]	28.1 [21.5]	–20.2 [–25.0]
As_4-Mg$(NH_3)_4$	35.8 [26.7]	17.1 [9.8]	30.8 [19.1]	3.0 [–4.5]	31.3 [23.4]	2.3 [–4.3]	30.2 [20.9]	–13.6 [–19.8]

Full Paper
doi.org/10.1002/ejic.202000422

the case of the reaction between **A** and C_2Cl_4 could be located in the isolated state. Instead, a nucleophilic attack at one of the carbon atoms of C_2Cl_4 was observed with concomitant loss of a chloride anion [Scheme 1 (b)]. The product of this reaction can be described as a vinyl-substituted tetrapnictide monoanion (**A-C_2Cl_3**). This result prompted us to consider this nucleophilic substitution reaction as alternative to the cycloaddition for all naked dianions **A** using a solvation model and Table 5 contains the obtained data. The calculations indicate that all reactions are strongly exergonic exceeding by far the ones for the cycloaddition reaction. Furthermore, the activation barriers are accessible at 240 K. The comparatively weak C–Cl bond (with respect to a C-F bond) and presumably high polarizability of the square-planar dianions **A** is likely an explanation for the ease by which this nucleophilic substitution reactions take place.

Table 5. Gibbs free energies of calculated transition states and products for the nucleophilic reactivity of **A** and **A-Mg$(NH_3)_4$** [PBE0-D3BJ/def2-TZVPP CPCM(ammonia), in kcal mol^{-1}] at 240 K. The sum of the Gibbs free energies of the respective starting materials for each reaction was taken as the reference.

	P_4^{2-}	As_4^{2-}	Sb_4^{2-}	Bi_4^{2-}	P_4-Mg$(NH_3)_4$	As_4-Mg$(NH_3)_4$
TS	18.3	17.9	18.6	14.9	29.4	29.1
A-C_2Cl_3	−34.1	−30.5	−28.1	−29.4	−32.4	−26.5

For the magnesium species **A-Mg$(NH_3)_4$** (**A** = P_4^{2-}, As_4^{2-}), both the activated complexes at the transition states and the products are destabilized compared to the cation-free dianions **A** on the biradicaloid reaction channels shown in Scheme 1a. This effect is especially strong in case of the transition states for the cycloadditions with the halogenated ethenes. An exception are the ethene addition products which are slightly stabilized (Table 4). Notably, in case of the magnesium species **A-Mg$(NH_3)_3$**, the barriers are lowered considerably and are accessible in the case of the reaction between ethene and tetrafluoroethene (Table 4, values in brackets). However, since the formation of **A-Mg$(NH_3)_3$** from **A-Mg$(NH_3)_4$** is endergonic (P: 4.2 kcal mol^{-1}, As: 5.7 kcal mol^{-1}), the total activation barrier is raised by the energy difference between these magnesium complexes. Therefore, they are not accessible at 240 K. Thus, magnesium complexes of tetrapnictide dianions do not seem to be promising candidates for reactivity studies. The same holds for the nucleophilic reactivity of these magnesium complexes. In comparison with the free dianions **A**, the reactions are slightly less exergonic, and the activation barriers are strongly raised (Table 5).

Conclusions

In summary, this study reveals several interesting aspects of the chemistry of tetrapnictide dianions. The results show that the butterfly isomer **B** might be accessible in the case of Sb and Bi in the presence of a dicationic counterion such as Mg^{2+}. In addition, multi-reference calculations have revealed the biradical character of the square-planar isomers **A**, which is comparable in magnitude to that of N_2S_2 (**1**). Overall, our calculations indicate that the biradical character of square-planar tetrapnictide dianions contributes to a certain extent to their reactivity. This is highlighted in the activation barriers of the addition reactions of dihydrogen and ethene derivatives to the tetrapnictides which decrease in the order Pn = P < As < Sb while the biradical character increases in this order. In particular, the predicted activation barrier for the addition reaction of P_4^{2-} and As_4^{2-} to tetrafluoroethene is rather low and accessible [19.3 kcal mol^{-1}; this corresponds to a rate constant of 1.3 L × (s mol)$^{-1}$ at 240 K] and the products are expected to be thermodynamically stable i.e. the reactions are calculated to be strongly exergonic and irreversible. The nucleophilic reaction channel as an alternative to the biradicaloid one leading to cycloaddition products is one side favored by the polarizability of Pn_4^{2-} which increases from P to Bi with concomitant lowering of the activation barriers. On the other side, the relatively weakness of the C-Cl bond and fugacity of Cl^- will favor this reaction type. The nucleophilic reactivity of the dianions towards electrophiles such as tetrachloroethylene may be of practical relevance. From a methodological aspect, our study also highlights the importance of the inclusion of solvation effects when dealing with the chemistry of such small and highly charged dianions.

Computational Details

All calculations were carried out with the ORCA[15] program package using the PBE0-D3BJ[16] functional and the def2-TZVPP[17] basis set. In order to cover relativistic effects for Pn = Sb and Bi, the respective effective core-potentials, def2-ECP,[18] were used. Solvent interactions were included for all structures by an implicit solvation model for ammonia (CPCM).[7] Approximate transition states were located using two-dimensional relaxed-surface scans which were then used for a subsequent saddle-point optimization. Frequency calculations were carried out to confirm the nature of stationary points found by geometry optimizations. It was found that DFT yields reliable energies by benchmarking against the very accurate DLPNO-CCSD(T) method[19] in conjunction with the ano-RCC-QZP[20] basis set. Here, a small mean absolute deviation (MAD) of 1.2 kcal mol^{-1} between the DFT and the DLPNO-CCSD(T) results was found (see the SI). The RIJK[21] approximation was used for DLPNO-CCSD(T) calculations whereas the RIJCOSX[22] approximation was used for DFT and CASSCF calculations. DFT orbitals served as initial guess for the CASSCF calculations. Topology analyses and calculations of the Shannon aromaticity index have been performed on the CASSCF electron densities of **A** using the program MultiWFN.[23]

Acknowledgments

Financial support by the ERC (CoG 772299) is gratefully acknowledged. We are especially thankful for the valuable comments of the reviewers. Open access funding enabled and organized by Projekt DEAL.

Keywords: Ab initio calculations · Density functional calculations · Heterocycles · Pnicogens · Radicals

[1] A. Cisar, J. D. Corbett, *Inorg. Chem.* **1977**, *16*, 2482–2487.
[2] a) S. C. Critchlow, J. D. Corbett, *Inorg. Chem.* **1984**, *23*, 770–774; b) F. Kraus, J. C. Aschenbrenner, N. Korber, *Angew. Chem. Int. Ed.* **2003**, *42*, 4030–4033; *Angew. Chem.* **2003**, *115*, 4162–4165; c) A. N. Kuznetsov, T. F. Fässler, *Z. Anorg. Allg. Chem.* **2002**, *628*, 2537–2541; d) N. Korber, M. Reil, *Chem. Commun.* **2002**, 84–85; e) T. Hanauer, F. Kraus, M. Reil, N. Korber, *Monatsh. Chem.* **2006**, *137*, 147–156; f) F. Kraus, T. Hanauer, N. Korber, *Inorg. Chem.* **2006**, *45*, 1117–1123.
[3] a) R. C. Burns, R. J. Gillespie, J. A. Barnes, M. J. McGlinchey, *Inorg. Chem.* **1982**, *21*, 799–807; b) R. A. J. Janssen, *J. Phys. Chem.* **1993**, *97*, 6384–6397; c) A. E. Kuznetsov, H.-J. Zhai, L.-S. Wang, A. I. Boldyrev, *Inorg. Chem.* **2002**, *41*, 6062–6070; d) Q. Jin, B. Jin, W. G. Xu, *Chem. Phys. Lett.* **2004**, *396*, 398–403; e) F. Kraus, N. Korber, *Chem. Eur. J.* **2005**, *11*, 5945–5959; f) J. O. C. Jiménez-Halla, E. Matito, J. Robles, M. Solà, *J. Organomet. Chem.* **2006**, *691*, 4359–4366; g) Z. Li, C. Zhao, L. Chen, *THEOCHEM* **2007**, *810*, 1–6; h) X. Wang, X. Chi, *Chin. J. Chem. Phys.* **2009**, *22*, 75–81; i) A. C. Tsipis, *Phys. Chem. Chem. Phys.* **2009**, *11*, 8244–8261; j) C. Wang, X. Zhang, J. Lu, Q. Li, *J. Mol. Model.* **2012**, *18*, 3577–3586; k) M. Perić, L. Andjelković, M. Zlatar, C. Daul, M. Gruden-Pavlović, *Polyhedron* **2014**, *80*, 69–80.
[4] a) E. Niecke, A. Fuchs, F. Baumeister, M. Nieger, W. W. Schoeller, *Angew. Chem. Int. Ed. Engl.* **1995**, *34*, 555–557; *Angew. Chem.* **1995**, *107*, 640–642; b) R. Evans, A. J. Downs, R. Köppe, S. C. Peake, *J. Phys. Chem. A* **2011**, *115*, 5127–5137; c) T. Beweries, R. Kuzora, U. Rosenthal, A. Schulz, A. Villinger, *Angew. Chem. Int. Ed.* **2011**, *50*, 8974–8978; *Angew. Chem.* **2011**, *123*, 9136–9140; d) A. Hinz, R. Kuzora, U. Rosenthal, A. Schulz, A. Villinger, *Chem. Eur. J.* **2014**, *20*, 14659–14673; e) A. Hinz, A. Schulz, A. Villinger, *Angew. Chem. Int. Ed.* **2015**, *54*, 668–672; *Angew. Chem.* **2015**, *127*, 678–682; f) A. Hinz, A. Schulz, A. Villinger, *Angew. Chem. Int. Ed.* **2016**, *55*, 12214–12218; *Angew. Chem.* **2016**, *128*, 12402; g) A. Hinz, A. Schulz, A. Villinger, *Chem. Commun.* **2016**, *52*, 6328–6331; h) Z. Li, X. Chen, D. M. Andrada, G. Frenking, Z. Benkö, Y. Li, J. R. Harmer, C.-Y. Su, H. Grützmacher, *Angew. Chem. Int. Ed.* **2017**, *56*, 5744–5749; *Angew. Chem.* **2017**, *129*, 5838–5843; i) Z. Li, Y. Hou, Y. Li, A. Hinz, X. Chen, *Chem. Eur. J.* **2018**, *24*, 4849–4855; j) W. W. Schoeller, *Eur. J. Inorg. Chem.* **2019**, *2019*, 1495–1506.
[5] a) F. Breher, *Coord. Chem. Rev.* **2007**, *251*, 1007–1043; b) T. Chu, G. I. Nikonov, *Chem. Rev.* **2018**, *118*, 3608–3680.
[6] a) R. D. Harcourt, T. M. Klapötke, A. Schulz, P. Wolynec, *J. Phys. Chem. A* **1998**, *102*, 1850–1853; b) H. M. Tuononen, R. Suontamo, J. Valkonen, R. S. Laitinen, *J. Phys. Chem. A* **2004**, *108*, 5670–5677; c) Y. Jung, T. Heine, P. v. R. Schleyer, M. Head-Gordon, *J. Am. Chem. Soc.* **2004**, *126*, 3132–3138; d) T. M. Klapötke, J. Li, R. D. Harcourt, *J. Phys. Chem. A* **2004**, *108*, 6527–6531; e) B. Braïda, A. Lo, P. C. Hiberty, *ChemPhysChem* **2012**, *13*, 811–819; f) R. D. Harcourt, *ChemPhysChem* **2013**, *14*, 2859–2864; g) F. E. Penotti, D. L. Cooper, P. B. Karadakov, *Int. J. Quantum Chem.* **2019**, *119*, e25845.
[7] M. Cossi, N. Rega, G. Scalmani, V. Barone, *J. Comput. Chem.* **2003**, *24*, 669–681.
[8] G. Van Zandwijk, R. A. J. Janssen, H. M. Buck, *J. Am. Chem. Soc.* **1990**, *112*, 4155–4164.
[9] J. M. Mercero, X. Lopez, J. E. Fowler, J. M. Ugalde, *J. Phys. Chem. A* **1997**, *101*, 5574–5579.
[10] a) M. Scheer, H. K. Haugen, D. R. Beck, *Phys. Rev. Lett.* **1997**, *79*, 4104–4107; b) R. C. Bilodeau, H. K. Haugen, *Phys. Rev. A* **2001**, *64*, 024501; c) C. W. Walter, N. D. Gibson, R. L. Field, A. P. Snedden, J. Z. Shapiro, C. M. Janczak, D. Hanstorp, *Phys. Rev. A* **2009**, *80*, 014501; d) R. J. Peláez, C. Blondel, M. Vandevraye, C. Drag, C. Delsart, *J. Phys. B* **2011**, *44*, 195009.
[11] S. Noorizadeh, E. Shakerzadeh, *Phys. Chem. Chem. Phys.* **2010**, *12*, 4742–4749.
[12] a) V.-A. Glezakou, S. T. Elbert, S. S. Xantheas, K. Ruedenberg, *J. Phys. Chem. A* **2010**, *114*, 8923–8931; b) E. Miliordos, K. Ruedenberg, S. S. Xantheas, *Angew. Chem. Int. Ed.* **2013**, *52*, 5736–5739; *Angew. Chem.* **2013**, *125*, 5848–5851; c) E. Miliordos, S. S. Xantheas, *J. Am. Chem. Soc.* **2014**, *136*, 2808–2817.
[13] a) L. Goerigk, S. Grimme, *Phys. Chem. Chem. Phys.* **2011**, *13*, 6670–6688; b) L. Goerigk, A. Hansen, C. Bauer, S. Ehrlich, A. Najibi, S. Grimme, *Phys. Chem. Chem. Phys.* **2017**, *19*, 32184–32215.
[14] C. Elschenbroich, *Organometallics: A Concise Introduction*, VCH Publishers Inc., New York, **1992**.
[15] a) F. Neese, *Wiley Interdiscip. Rev.: Comput. Mol. Sci. Wiley Interdiscip. Rev. Comput. Mol. Sci.* **2012**, *2*, 73–78; b) F. Neese, *Wiley Interdiscip. Rev.: Comput. Mol. Sci. Wiley Interdiscip. Rev. Comput. Mol. Sci.* **2018**, *8*, e1327.
[16] a) C. Adamo, V. Barone, *J. Chem. Phys.* **1999**, *110*, 6158–6170; b) S. Grimme, J. Antony, S. Ehrlich, H. Krieg, *J. Chem. Phys.* **2010**, *132*, 154104; c) S. Grimme, S. Ehrlich, L. Goerigk, *J. Comput. Chem.* **2011**, *32*, 1456–1465.
[17] F. Weigend, R. Ahlrichs, *Phys. Chem. Chem. Phys.* **2005**, *7*, 3297–3305.
[18] B. Metz, H. Stoll, M. Dolg, *J. Chem. Phys.* **2000**, *113*, 2563–2569.
[19] a) C. Riplinger, B. Sandhoefer, A. Hansen, F. Neese, *J. Chem. Phys.* **2013**, *139*, 134101; b) D. G. Liakos, M. Sparta, M. K. Kesharwani, J. M. L. Martin, F. Neese, *J. Chem. Theory Comput.* **2015**, *11*, 1525–1539.
[20] a) P.-O. Widmark, P.-Å. Malmqvist, B. O. Roos, *Theor. Chim. Acta* **1990**, *77*, 291–306; b) B. O. Roos, V. Veryazov, P.-O. Widmark, *Theor. Chem. Acc.* **2004**, *111*, 345–351; c) B. O. Roos, R. Lindh, P.-Å. Malmqvist, V. Veryazov, P.-O. Widmark, *J. Phys. Chem. A* **2004**, *108*, 2851–2858.
[21] F. Weigend, *Phys. Chem. Chem. Phys.* **2002**, *4*, 4285–4291.
[22] F. Neese, F. Wennmohs, A. Hansen, U. Becker, *Chem. Phys.* **2009**, *356*, 98–109.
[23] T. Lu, F. Chen, *J. Comput. Chem.* **2012**, *33*, 580–592.

Received: April 30, 2020